

**A peer-reviewed version of this preprint was published in PeerJ on 4 April 2019.**

[View the peer-reviewed version](https://peerj.com/articles/6689) (peerj.com/articles/6689), which is the preferred citable publication unless you specifically need to cite this preprint.

Sharanowski BJ, Peixoto L, Dal Molin A, Deans AR. 2019. Multi-gene phylogeny and divergence estimations for Evaniidae (Hymenoptera) PeerJ 7:e6689 <https://doi.org/10.7717/peerj.6689>

# Multi-gene phylogeny and divergence estimations for Evaniidae (Hymenoptera)

Barbara J Sharanowski<sup>1</sup>, Leanne Peixoto<sup>2</sup>, Anamaria Dal Molin<sup>3</sup>, Andrew R Deans<sup>Corresp.</sup><sup>4</sup>

<sup>1</sup> Department of Biology, University of Central Florida, Orlando, Florida, United States

<sup>2</sup> Department of Agroecology, Aarhus University, Aarhus, Denmark

<sup>3</sup> Departamento de Ciências Biológicas, Universidade Federal do Espírito Santo, Vitória, ES, Brazil

<sup>4</sup> Frost Entomological Museum, Department of Entomology, Pennsylvania State University, University Park, PA, United States

Corresponding Author: Andrew R Deans

Email address: adeans@psu.edu

Ensign wasps (Hymenoptera: Evaniidae) develop as predators of cockroach eggs (Blattodea), have a wide distribution and exhibit numerous interesting biological phenomena. The taxonomy of this lineage has been the subject of several recent, intensive efforts, but the lineage lacked a robust phylogeny. In this paper we present a new phylogeny, based on increased taxonomic sampling and data from six molecular markers (mitochondrial *16S* and *COI*, and nuclear markers *28S*, *RPS23*, *CAD*, and *AM2*), the latter used for the first time in phylogenetic reconstruction. Our intent is to provide a robust phylogeny that will stabilize and facilitate revision of the higher-level classification. We also show the continued utility of molecular motifs, especially the presence of an intron in the *RPS23* fragments of certain taxa, to diagnose evaniid clades and assist with taxonomic classification. Furthermore, we estimate divergence times among evaniid lineages for the first time, using multiple fossil calibrations. Evaniidae radiated primarily in the Early Cretaceous (134.1-141.1 Mya), with and most extant genera diverging near the K-T boundary. The estimated phylogeny reveals a more robust topology than previous efforts, with the recovery of more monophyletic taxa and better higher-level resolution. The results facilitate a change in ensign wasp taxonomy, with *Parevania*, **syn. nov.**, and *Papatuka*, **syn. nov.** becoming junior synonyms of *Zeuxevania*, and *Acanthinevania*, **syn. nov.** being designated as junior synonym of *Szepligetella*. We transfer 30 species to *Zeuxevania*, either reestablishing past combinations or as new combinations. We also transfer 20 species from *Acanthinevania* to *Szepligetella* as new combinations.

# 1 Multi-gene phylogeny and divergence 2 estimations for Evaniidae (Hymenoptera)

3 Barbara J. Sharanowski<sup>1</sup>, Leanne Peixoto<sup>2</sup>, Anamaria Dal Molin<sup>3</sup>, and  
4 Andrew R. Deans<sup>4</sup>

5 <sup>1</sup>University of Central Florida, Department of Biology, 4110 Libra Drive, BIO 301,  
6 Orlando, Florida, USA 32816-2368

7 <sup>2</sup>Aarhus University, Department of Agroecology, Aarhus, Denmark, AU Foulum,  
8 Blichers Allé 20 8830 Tjele

9 <sup>3</sup>Depto. Ciências Biológicas, Universidade Federal do Espírito Santo, Vitória, ES, Brazil

10 <sup>4</sup>Frost Entomological Museum, Department of Entomology, 501 ASI Building,  
11 Pennsylvania State University, University Park, PA USA 16802

12 Corresponding author:

13 Andrew R. Deans<sup>4</sup>

14 Email address: adeans@psu.edu

## 15 ABSTRACT

16 Ensign wasps (Hymenoptera: Evaniidae) develop as predators of cockroach eggs (Blattodea), have a  
17 wide distribution and exhibit numerous interesting biological phenomena. The taxonomy of this lineage  
18 has been the subject of several recent, intensive efforts, but the lineage lacked a robust phylogeny. In this  
19 paper we present a new phylogeny, based on increased taxonomic sampling and data from six molecular  
20 markers (mitochondrial *16S* and *COI*, and nuclear markers *28S*, *RPS23*, *CAD*, and *AM2*), the latter  
21 used for the first time in phylogenetic reconstruction. Our intent is to provide a robust phylogeny that  
22 will stabilize and facilitate revision of the higher-level classification. We also show the continued utility  
23 of molecular motifs, especially the presence of an intron in the *RPS23* fragments of certain taxa, to  
24 diagnose evaniid clades and assist with taxonomic classification. Furthermore, we estimate divergence  
25 times among evaniid lineages for the first time, using multiple fossil calibrations. Evaniidae radiated  
26 primarily in the Early Cretaceous (134.1–141.1 Mya), with and most extant genera diverging near the  
27 K-T boundary. The estimated phylogeny reveals a more robust topology than previous efforts, with the  
28 recovery of more monophyletic taxa and better higher-level resolution. The results facilitate a change in  
29 ensign wasp taxonomy, with *Parevania*, **syn. nov.**, and *Papatuka*, **syn. nov.** becoming junior synonyms  
30 of *Zeuxevania*, and *Acanthinevania*, **syn. nov.** being designated as junior synonym of *Szepligetella*. We  
31 transfer 30 species to *Zeuxevania*, either reestablishing past combinations or as new combinations. We  
32 also transfer 20 species from *Acanthinevania* to *Szepligetella* as new combinations.

## 33 INTRODUCTION

34 Ensign wasps (Hymenoptera: Evaniidae) are common, nearly cosmopolitan, and include approximately  
35 500 extant species in 21 genera, although many species remain to be described (Deans, 2005). Their  
36 biology lies at the precipice between wasps that provision their young with prey and parasitic wasps that  
37 deposit their offspring to feed on one host. A female evaniid wasp lays a single egg within a cockroach  
38 egg case and their offspring feeds on the unhatched cockroach eggs. Because their larvae feed on multiple  
39 hosts, ensign wasps are regarded as predators as opposed to parasitoids (Huben, 1995). However, the  
40 intimate association that larval evaniids have with their prey is much more reminiscent of parasitoid  
41 behavior. Despite these interesting biological features, there is scant research aimed at understanding  
42 their evolution and natural history. This predicament remains, in part, due to ongoing instability in their  
43 classification and the lack of robust diagnostic tools and inadequate taxon descriptions. Taxonomic work  
44 over the last 20 years, however, including a key to genera (Deans and Huben, 2003), a comprehensive  
45 species catalog (Deans, 2005, treating all ca. 500 species), descriptions of fossils (Deans et al., 2004;  
46 Jennings et al., 2013, 2012, 2004), and updated (Deans and Kawada, 2008) and semantically-enhanced

47 species-level revisions (Balhoff et al., 2013; Mikó et al., 2014) have substantially increased the potential  
48 for research on these insects.

49 Deans et al. (2006) also published the first phylogeny of the family, which was an attempt to test the  
50 historic generic and tribal classifications. Of the 17 included genera, four were represented by single  
51 specimens: *Papatuka* Deans, *Rothevania* Huben (monotypic), *Thaumatevania* Ceballos (monotypic),  
52 and *Trissevania* Kieffer. Six genera were found to be monophyletic in both a parsimony and Bayesian  
53 analysis, including: *Acanthinevania* Bradley, *Decevania* Huben, *Evania* Fabricius, *Evaniscus* Szépligeti,  
54 *Micrevania* Benoit, and *Semaemyia* Bradley. Although *Prosevania* Kieffer was always recovered,  
55 with one possibly misplaced specimen of *Szepligetella* Bradley, it is likely that *Prosevania* may also  
56 be monophyletic. Several other genera were consistently recovered as paraphyletic or in unresolved  
57 polytomies, including *Brachygaster* Leach, *Evaniella* Bradley, *Hyptia* Illiger, *Szepligetella* Bradley,  
58 *Parevania* Kieffer, and *Zeuxevania* Kieffer. The latter two genera were consistently recovered in a clade  
59 with *Papatuka* Deans, and Deans et al. (2006) suggested that these taxa may be congeneric based on  
60 the molecular results and inconsistencies in the morphological character that separates these two genera  
61 (presence of fore wing 1RS in *Parevania*). They also suggested *Evaniella* may be monophyletic as it  
62 was consistently recovered with the exception of one aberrant taxon, since described as its own genus  
63 (*Alobevania* Deans and Kawada, 2008)).

64 The only tribal classification put forth for Evaniidae was by Bradley (1908), who suggested two  
65 tribes for the ten genera described at the time: Hyptiini (including *Evaniella*, *Evaniscus*, *Hyptia*, *Pare-*  
66 *vania*, *Semaemyia*, and *Zeuxevania*) and Evaniini (including *Acanthinevania*, *Evania*, *Prosevania*, and  
67 *Szepligetella*). This tribal classification was not supported by Deans et al. (2006). There was not enough  
68 resolution to confidently resolve relationships among evaniid genera to develop a better tribal classification.  
69 Deans et al. (2006) did suggest that the New World taxa with reduced wing venation (including *Evaniscus*,  
70 *Decevania*, *Hyptia*, *Rothevania*, and *Semaemyia*) were monophyletic and could represent a tribe.

71 The poorly resolved phylogenies published by Deans et al. (2006) may be attributed to low taxonomic  
72 sampling, as only 54 ingroup taxa were included, or, more likely, a lack of informative sites in the sequence  
73 data. The resulting “backbone polytomy”, where higher-level classifications remain elusive, is common in  
74 other phylogenies of Hymenoptera that use the same or similar sets of genes (Dowton and Austin, 2001;  
75 Mardulyn and Whitfield, 1999; Pitz et al., 2007). Divergence times for members of Evaniidae have not  
76 been estimated before. Several recent studies on Hymenoptera have estimated stem-age divergences for  
77 Evanioidea ranging from 175 Ma to 221 Ma (Ronquist et al., 2012a; Zhang et al., 2015; Peters et al.,  
78 2017; Branstetter et al., 2017). Unfortunately, the small sample size for Evanioidea in all of these studies  
79 (1–3 exemplars) and uncertainty in phylogenetic relationships of Evanioidea within Hymenoptera resulted  
80 in wide confidence intervals around the estimates. Based on all fossils placed within Evanioidea, it is  
81 likely that the superfamily diversified in the Middle Jurassic but may have originated as early as the late  
82 Triassic (Li et al., 2018).

83 Here we attempt to gain a better understanding of higher-level relationships among genera and better  
84 test the monophyly of genera, using an increased taxonomic and genetic sampling dataset, including  
85 a handful of new protein-coding genes. Our intent is to provide a robust phylogeny that will stabilize  
86 and facilitate revision of the higher-level classification. We also show the continued utility of molecular  
87 motifs, first described for Evaniidae by Deans et al. (2006), to diagnose clades and assist with taxonomic  
88 classification. Furthermore, we estimate divergence times among evaniid lineages for the first time, using  
89 multiple fossil calibrations to understand of the timing of diversification in Evaniidae.

## 90 MATERIALS AND METHODS

### 91 Taxon sampling

92 A list of taxa and sequences utilized in this study is presented in Table 1 (more details in Table S1).  
93 Exemplars were obtained for 89 evaniid specimens, across 17 genera, and five outgroup taxa, including  
94 two species of *Gasteruption* (Gasteruptionidae) and three species of *Pristaulacus* (Aulacidae), for a total  
95 of 94 taxa. All evaniid genera were represented except four rare genera: *Afrevania*, *Brachevania*,  
96 *Thaumatevania*, and *Vernevania*. We were only able to include one representative of *Alobevania* and  
97 *Rothevania* (monotypic), and *Papatuka*. Where possible, sampling was increased for genera that were  
98 previously recovered as paraphyletic by Deans et al. (2006).

taxon	Ext.	DV#	28S	AM2	CAD1	CAD2	RPS23	COI	16S
<i>Gasteruption</i> 300	300		X		X	X	X	X	D
<i>Gasteruption</i> 244	244		X		X		X	X	
<i>Pristaulacus strangaliae</i>	176			X			X	X	
<i>Pristaulacus fasciatus</i>	299							X	
<i>Pristaulacus</i> 21	306	21	D				X	D	D
<i>Acanthinevania</i> 240	240		X	X	X	X	X	X	
<i>Acanthinevania</i> 242	242		X	X	X	X	X		
<i>Acanthinevania princeps</i>	246		X		X	X	X	X	
<i>Acanthinevania</i> 001	271	001	D	X	X	X	X	D	D
<i>Acanthinevania</i> 033	289	033	D	X	X	X	X	D	D
<i>Acanthinevania</i> 049	292	049	D	X	X	X	X	D	D
<i>Alobevania gattiae</i>	200	039	D	X	X	X		X	D
<i>Brachygaster minutus</i>	273	030	X		X	X	X	D	D
<i>Brachygaster minutus</i>	512				X	X		X	
<i>Brachygaster</i> 037	286		D		X		X		D
<i>Brachygaster</i> 050	290		D				X		D
<i>Decevania</i> 502	502				X	X			
<i>Decevania</i> 513	513			X				X	
<i>Decevania</i> 004	274	004	D	X		X	X	D	D
<i>Decevania</i> 005	301	005	D				X		D
<i>Decevania</i> 063	296	063	D	X	X	X	X	D	D
<i>Evania</i> 175	175		X				X	X	
<i>Evania albofacialis</i>	275	020	D		X	X	X	D	D
<i>Evania appendigaster</i>	207	046	D		X	X	X	D	D
<i>Evania</i> 496	496		X			X	X	X	
<i>Evania</i> 002	189	002	D		X	X		D	D
<i>Evaniella</i> 230	230		X	X	X	X	X	X	
<i>Evaniella</i> 234	234		X	X		X	X	X	
<i>Evaniella</i> 237	237			X	X			X	
<i>Evaniella</i> 485	485			X	X	X	X		
<i>Evaniella</i> 486	486			X	X		X		
<i>Evaniella</i> 493	493				X		X	X	
<i>Evaniella semaeoda</i>	220	058	D				X	D	D
<i>Evaniella</i> 019	192	019	D	X	X		X	D	
<i>Evaniella</i> 025	307	025	D		X		X	D	D
<i>Evaniella</i> 045	206	045	D	X	X		X		D
<i>Evaniscus marginatus</i>	213	052	D				X		D
<i>Evaniscus rufithorax</i>	206		D			X	X	X	D
<i>Hyptia</i> 232	232			X	X	X	X	X	
<i>Hyptia</i> 487	487			X				X	
<i>Hyptia</i> 501	501			X	X			X	
<i>Hyptia</i> 511	511			X	X			X	
<i>Hyptia amazonica</i>	235				X	X		X	
<i>Hyptia floridana</i>	291	009	D	X	X	X		D	D
<i>Hyptia</i> 007	302	007	D		X		X	D	D
<i>Hyptia</i> 008	303	008	D				X	D	D
<i>Micrevania difficilis</i>	283	006	D		X	X		X	D
<i>Micrevania</i> 061	288	061	D	X		X		D	D
<i>Micrevania</i> 066	298	066	D			X		D	D
<i>Micrevania</i> 026	308	026	D			D		D	D
<i>Papatuka capensis</i>	227	065	D		X	X	X	X	D
<i>Parevania</i> 172	172		X	X	X		X		
<i>Parevania</i> 174	174		X	X			X	X	

Continued on next page

Table 1 – Continued from previous page

taxon	Ext.	DV#	28S	AM2	CAD1	CAD2	RPS23	COI	16S
<i>Parevania</i> 041	295	041	D	X	X	X	X	D	D
<i>Parevania</i> 057	219	057	D	X	X	X	X		D
<i>Parevania</i> 064	276	064	D		X	X	X	D	D
<i>Prosevania fuscipes</i>	224	062	D			X		X	D
<i>Prosevania</i> 497	497		X	X	X	X		X	
<i>Prosevania</i> 498	498				X			X	
<i>Prosevania</i> 508	508							X	
<i>Prosevania</i> 027	309	027	D	X		X		X	D
<i>Prosevania</i> 034	277	034	D					D	D
<i>Prosevania</i> 036	284	036	D		X	X		X	D
<i>Prosevania</i> 044	205	044	D	X	X	X	X	D	D
<i>Rothevania valdivianus</i>	239	048	D	X	X	X		D	D
<i>Semaeomyia</i> 489	489				X	X	X	X	
<i>Semaeomyia</i> 509	509		X			X	X	X	
<i>Semaeomyia</i> 510	510		X			X	X	X	
<i>Semaeomyia leucomelas</i>	305	016	D			X	X	D	D
<i>Semaeomyia</i> 012	197	012	D		X	X		D	D
<i>Semaeomyia</i> 051	279	051	D			X	X	D	D
<i>Semaeomyia</i> 059	293	059	D	X		X	X	D	D
<i>Szepligetella</i> 170	170				X		X	X	
<i>Szepligetella</i> 231	231		X		X	X	X	X	
<i>Szepligetella</i> 233	233		X	X	X	X	X	X	
<i>Szepligetella</i> 236	236		X	X	X	X		X	
<i>Szepligetella</i> 238	238		X	X	X	X	X	X	
<i>Szepligetella</i> 241	241				X	X	X	X	
<i>Szepligetella</i> 243	243		X	X	X		X	X	
<i>Szepligetella</i> 247	247				X		X	X	
<i>Szepligetella</i> 248	248		X		X		X	X	
<i>Szepligetella sericea</i>	297					X	X	X	
<i>Szepligetella</i> 047	208	047	D	X	X		X	D	D
<i>Szepligetella</i> 055	280	055		X	X		X	D	D
<i>Szepligetella</i> 056	294	056	D	X	X	X	X	X	D
<i>Szepligetella</i> 285	285			X	X	X	X	X	
<i>Trissevania anemotis</i>	282	038	D	X		X	X	D	D
<i>Trissevania</i> 507	507					X			
<i>Zeuxevania</i> 499	499				X	X			
<i>Zeuxevania</i> 500	500				X	X		X	
<i>Zeuxevania</i> 503	503					X			
<i>Zeuxevania</i> 505	505		X		X	X	X	X	
<i>Zeuxevania</i> 015	191	015	D		X			D	D
<i>Zeuxevania splendidula</i>	312	031	D		X	X	X	X	D
% amplified			71	44	66	64	67	86	50
% parsimony-informative			40	44	49	53	35	60	40

**Table 1.** Taxonomic and genetic sampling. Exemplars used by Deans et al. (2006) are listed with the reference from that paper (DV#) beside the internal voucher number (Ext.) Genes for each taxon are marked with an **X** if amplified in this study and **D** if amplified by Deans et al. (2006). Gene codes: 28S = 28S rDNA; AM2 = alpha-mannosidase II; CAD1 and CAD2 = carbamoyl-phosphate synthetase-aspartate transcarbamoylase-dihydroorotase (CAD) (for amplicon regions for each segment, see Figure 1); RPS23 = Ribosomal Protein S23; COI = cytochrome oxidase I; 16S = 16S rDNA.

99

100 Each exemplar not identified to species represents a putative morphospecies, as many species remain

101 undescribed. Several DNA extracts and some sequences were used from Deans et al. (2006), as indicated  
102 in Table 1. Vouchers were deposited at the Frost Entomological Museum, at The Pennsylvania State  
103 University, or in repositories stipulated by collecting permits and/or loan agreements. See supplementary  
104 CSV file (EvaniidPhylogenyVouchers.csv).

### 105 Gene selection

106 We utilized DNA from six different genes, including two mitochondrial (mt) genes (16S ribosomal DNA  
107 (*16S*) and cytochrome c oxidase I (*COI*)) and four nuclear genes (28S ribosomal DNA (*28S*), ribosomal  
108 protein S23 (*RPS23*), carbamoyl-phosphate synthetase-aspartate transcarbamoylase-dihydroorotase (*CAD*)  
109 and alpha-mannosidase II (*AM2*)). Diagrams of the gene structures of *CAD*, *RPS23*, and *AM2* are  
110 presented in Figure 1. The diagrams were produced based on annotations of the genomic reference  
111 sequences from *Apis mellifera* Linnaeus, 1758 (NCBI RefSeq ID: GCF\_000002195.4) and *Nasonia*  
112 *vitripennis* (Ashmead, 1904) (NCBI RefSeq ID: GCF\_000002325.3), visualized in NCBI's Sequence  
113 Viewer (<http://www.ncbi.nlm.nih.gov/tools/sviewer>) and Geneious v.6.0.6 (Biomatters  
114 Ltd.) The annotations include information on the introns, exons, organization of coding regions and  
115 protein product features. Conserved domains in the protein products were also identified via a BLASTx  
116 search (Altschul et al., 1990) against NCBI's Conserved Domains Database (CDD) (Marchler-Bauer  
117 et al., 2015). The genetic regions corresponding to the identified domains are included for reference in  
118 the diagrams as well as the primers used in this study (primer sequences are listed in Table S2). Further  
119 background about the three protein coding genes is provided below since the amplified regions or genes  
120 utilized are novel for phylogenetic studies. All sequences are available in NCBI's Genbank (<https://www.ncbi.nlm.nih.gov/genbank/>)  
121 under accession numbers KY082187–KY082565.

### 122 CAD

123 *CAD* is a long and complex gene which codes a “fusion” protein, that is, a protein with multiple  
124 enzymatic activities: glutamine-amidotransferase (GATase), carbamoylphosphate synthetase (CPSase),  
125 dihydroorotase (DHOase) and aspartate/ornithine transcarbamoylase (ATCase/OTC). There are 26 exons  
126 and 25 introns in both *Apis* and *Nasonia*, although intron loss has been reported in the CPSase small chain  
127 region in some Braconidae (Sharanowski et al., 2011). CPSase is divided in two domains: one for a short  
128 chain, which includes GATase, and one for a long chain. The long chain is also subdivided, consisting  
129 of two subunits (N-terminal + ATP-binding region), one oligomerization domain, and one MGS-like  
130 (methylglyoxal synthetase-like) domain. These two CPSase chains are coded by 14 exons. Various  
131 segments of this gene have been used in other phylogenetic studies of insects, particularly for lineages  
132 diversifying within the last 150 million years (Danforth et al., 2006; Moulton and Wiegmann, 2004;  
133 Winterton and De Freitas, 2006). The regions we analyzed are within the CPSase domains, extending  
134 between exons 3 to 5 (Figure 1A).

### 135 RPS23

136 Ribosomal protein S23 (Figure 1B) is part of the small ribosomal subunit (Wool, 1979). It has a binding  
137 site for mRNA and is associated with the eukaryotic initiation factor of the translation process (NCBI-  
138 CDD:cd03367). This gene has been previously used in macro-evolutionary phylogenetic studies on  
139 Hymenoptera (Sharanowski et al., 2010) and Arthropoda (Aleshin et al., 2009; Timmermans et al., 2008)  
140 and as an EPIC (exon-primed, intron-crossing) marker for population-level studies (Lohse et al., 2011,  
141 2010). RPS23 is well conserved in sequence and structure across Hymenoptera, with the variation  
142 concentrated in the introns. In both *Apis* and *Nasonia*, there are three exons (3bp, 159bp, and 270bp  
143 in length) and 2 introns (339bp and 84bp in *Apis*; 353bp and 79bp in *Nasonia*). The amplified region  
144 covers the downstream region of exon 2, full intron 2, and about half of exon 3, which contains the  
145 aminoacyl-tRNA interaction site and therefore is expected to be conserved.

### 146 AM2

147 We performed sequence similarity searches with tBLASTx (Altschul et al., 1990), using Hymenopteran  
148 expressed sequence tags (ESTs) from Sharanowski et al. (2010) against proteins of *Apis mellifera* and  
149 *Nasonia vitripennis*. Our search focused on genes with regions of variability (for putative phylogenetic  
150 signal), limited introns and relatively long exons, and regions of sequence conservation (for priming sites).  
151 Alpha-mannosidase II is a glycoside hydrolase involved in the catabolism of carbohydrates (Gonzalez and  
152 Jordan, 2000) and has not been explored for phylogenetic studies. There has been a shift in the placement  
153 of the second intron between *Nasonia* and *Apis* (Figure 1C), and thus we labeled the exons 2a and 2b

154 to demonstrate the homology with labeled exon 3 in both taxa. Three main protein domain regions are  
155 identifiable in the reference sequences: (1) an N-terminal catalytic domain of Golgi alpha-mannosidase II,  
156 which is entirely in exon 2a in *Apis*, but overlaps the second intron in *Nasonia*, and therefore also lies in  
157 exon 2b; (2) a middle domain, which is located in exon 3; and (3) and a C-terminal, which is located in  
158 exon 4 (Figure 1C). The amplified area is contained in the region that corresponds to the N-terminal in  
159 *Apis*, ending before the second intron (Figure 1C). No intron was amplified in the evanioid taxa used in  
160 this study, and thus the gene structure is more similar to *Apis* in the amplified region.

## 161 Extraction and Sequencing

162 Extraction of genomic DNA was performed following the manufacturer's protocols using the DNeasy™  
163 Tissue Kit (Qiagen, USA). Exemplars were either whole body extracted or only the separated thorax  
164 and metasoma were used as the use of the head often resulted in low DNA concentrations in Evaniids.  
165 *COI* was amplified using the protocols outlined in Schulmeister et al. (2002), with the primers developed  
166 for that study or using the universal primers developed by Folmer et al. (1994) and following protocols  
167 outlined in Namin et al. (2014) (Table S2). Sequences for 16S mitochondrial rDNA were used from Deans  
168 et al. (2006), which were based on primers and protocols developed in previous studies (Dowton and  
169 Austin, 1994; Whitfield, 1997). Amplification of the D2-D3 region of 28S was performed using either  
170 primers developed by Dowton and Austin (2001) or primers newly developed for this study (Table S2),  
171 due to difficulty with amplification of some taxa. *CAD* sequences were amplified in two discontinuous  
172 fragments using newly developed primers (Figure 1; Table S2: *CAD1*, *CAD2*). For *CAD1*, three reverse  
173 primers were developed to either reduce degeneracy or due to amplification difficulties in some taxa, and  
174 a touchdown protocol was also used to increase specificity of the reaction (Table S2). For *CAD2*, two sets  
175 of primers were developed, the second set (CAD-Amel379F/CAD-Amel479R) slightly internal to the  
176 first (CAD-Amel368F/CAD-Amel482R). If no amplification product was achieved with the first set of  
177 primers, the second set was used alone or as a nested re-amplification of the product obtained with the  
178 first set. *RPS23* was amplified using primers developed by Lohse et al. (2011) and in conjunction with  
179 a second newly developed reverse primer and amplified with a touchdown protocol (Figure 1B; Table  
180 S2). Primers were also designed to amplify AM2, with an internal forward primer (AM2-Amel1356F)  
181 amplifying a much shorter fragment (Figure 1C, Table S2), which increased the number of taxa for which  
182 we achieved amplification success.

183 All PCR amplifications were carried out using 0.2–1 μg DNA extract, 1× Standard Taq Buffer (New  
184 England Biolabs, USA) (10 mM Tris-HCl, 50 mM KCl, 1.5 mM MgCl<sub>2</sub>), 200 μm dNTP, 4 mM MgSO<sub>4</sub>,  
185 400 nM of each primer, 1 unit of Taq DNA polymerase (New England Biolabs, USA) and purified water to  
186 a final volume of 25 μL. PCR products were visualized on a 1% agarose gel. Occasionally 5% Dimethyl  
187 sulfoxide (DMSO, Sigma-Aldrich, USA) was added as a PCR additive when non-specific bands occurred.  
188 This additive has been shown to increase PCR yield with GC-rich templates (Farell and Alexandre, 2012).  
189 Nested re-amplifications were performed using 0.5 μL of PCR product as DNA template (concentrations  
190 varied depending on first PCR reaction success). PCR purification was performed using ExoSAP-IT  
191 (Affymetrix, USA) following the manufacturer's instructions, except using 25% of the suggested reagent  
192 amount. If double bands were visualized on the gel following PCR, a subsequent 50 μL reaction was run  
193 on gel cut bands, the product ran on a 2.5% agarose gel, and purified using the QIAquick Gel Extraction  
194 Kit (Qiagen, USA) following the manufacturer's protocols. Sequencing was carried out using the BigDye  
195 Terminator v 3.1 Cycle Sequencing Kit (Applied Biosystems, U.S.A.), with reaction products sequenced  
196 on an Applied Biosystems 3730xl DNA Analyzer at the Genomic Sciences Laboratory, North Carolina  
197 State University. Contigs were assembled and trimmed for quality using Geneious.

## 198 Sequence alignment

199 The protein-coding genes were aligned by translating the sequences and setting the correct reading frame  
200 in BioEdit (Hall, 1999). Sequences were then aligned as proteins using MAFFT (Katoh and Standley,  
201 2013) on the EMBL-EBI webserver (Li et al., 2015) under default settings and then back translated  
202 to nucleotides. Introns present in *CAD1* and *RPS23* were excluded from the dataset prior to multiple  
203 sequence alignment. Ribosomal DNA sequences were aligned following secondary structure models  
204 developed by Gillespie et al. (2005a,b) and modified by Deans et al. (2006) for Evaniidae. Regions of  
205 ambiguous alignment (RAA), expansion and contraction (REC), and slipped-strand compensation (RSC)  
206 were excluded from the analysis, following Deans et al. (2006). For analysis of sequence motifs, intron



207 were aligned using MAFFT with a gap opening penalty of 2 and gap extension penalty of 0.5 to limit  
208 excessive gaps in the alignment.

### 209 **Phylogenetic analyses**

210 The optimal partitioning scheme and models of evolution for the concatenated analysis were determined  
211 using PartitionFinder v.1.1.1 (Lanfear et al., 2012). Character sets were predefined by gene, and by codon  
212 position for the 5 protein-coding genes for a total of 17 partitions (*CAD1* and *CAD2* were partitioned  
213 separately). The Bayesian information criterion was used to select among models implemented in  
214 MrBayes version 3.2 Ronquist et al. (2012b), with the greedy search algorithm and branch lengths  
215 unlinked. The optimal scheme included two partitions. The first partition included the 3rd codon positions  
216 for *CAD1*, *CAD2*, *AM2*, and *RPS23* under the Hasegawa-Kishino-Yano model (Hasegawa et al., 1985).  
217 The remaining 13 predefined partitions were included together under the general time reversible model  
218 (GTR). Both partitions included a parameter for invariant sites and rate heterogeneity modeled under a  
219 gamma distribution. We observed notable differences in nucleotide composition across taxa for some  
220 genes (calculated in MEGA v.6 Tamura et al., 2013), and thus, tested for base composition homogeneity  
221 using chi-square tests in PAUP\* (Swofford, 2002) (Supplementary Material Table S3). For *CAD1* and  
222 *RPS23* the intron was removed.

223 Phylogenies were estimated using MrBayes 3.2, either on the CIPRES Science Gateway (Miller et al.,  
224 2010) or the ComputeCanada WestGrid computational facility. Parameters were unlinked and site specific  
225 rates were allowed to vary across partitions. Analyses were performed with two independent searches  
226 and four chains. All concatenated analyses were run for 10 million generations, sampling every 2000th  
227 generation. Individual gene trees were analyzed with 5 million generations, sampling every 1000th.  
228 Convergence diagnostics, stationarity, and appropriate mixing were assessed with Tracer v1.6 (Rambaut  
229 and Drummond, 2009), and a suitable burn-in was chosen based on the parameter values. Trees from  
230 the posterior distribution were summarized post burn-in with a majority rule consensus and manipulated  
231 for better visualization using FigTree v.1.3.1 (Rambaut, 2012) and modified for publication using Adobe  
232 Illustrator (Adobe Systems, Inc. San Jose, CA). The final nexus file is available through Penn State's  
233 ScholarSphere repository (DOI: 10.18113/S1D06H).

### 234 **Divergence time estimations**

235 An uncorrelated log-normal relaxed clock as implemented in the program BEAUTi and BEAST v.1.8.2  
236 (Drummond et al., 2002, 2012) was used to estimate divergence times. The same partitions and models  
237 of molecular evolution were applied to each partition as in the phylogenetic analysis. We utilized the  
238 Birth-Death process for incomplete sampling (Stadler, 2009) and started with a random tree. Only  
239 the calibration for the entire ingroup (Evaniidae) was constrained to be monophyletic which was well  
240 supported from the Bayesian analysis.

241 We utilized six fossil calibration points with each fossil assigned to the crown group for which they  
242 belonged (see Fossil Calibrations in Supplementary Material) (Brues, 1933; Nel et al., 2002; Peñalver et al.,  
243 2010; Jennings et al., 2004, 2013; Jennings and Krogmann, 2009; Rasnitsyn et al., 1998; Sawoniewicz  
244 and Kupryjanowicz, 2003). We performed two separate analyses to examine uncertainty with respect to  
245 maximum bounds for clade ages. For the first analysis we used log-normal distributions. The age of the  
246 fossil determined the hard minimum bound, as the clade to which it belongs must be at least that old. We  
247 then chose a mean and standard deviation so that the 95% highest priority density interval (95% HDP)  
248 for the divergence estimation of the clade was from 2 to 25 million years prior to the age of the fossil. The 25  
249 million year demarcation is arbitrary, but it seems reasonable and follows Cardinal and Danforth (2013).  
250 For the second analysis we chose hard maximum bounds based on previous knowledge of the fossil record  
251 and the evolutionary relationships among the included taxa, which are justified (Supplementary Material  
252 – Fossil Calibrations) for each calibration. Generally, we chose the mean as the average between the  
253 hard minimum and maximum bounds and then set the standard deviation so that the 95% HDP spanned  
254 the range from the minimum to the maximum bound. For both analyses, initial values were set to the  
255 mean and the ucl.d.mean prior was set to exponential with a mean of 0.05. Although these values are  
256 somewhat arbitrary, according to the authors of the program, they are unlikely to have an effect on  
257 the analysis (Drummond and Rambaut, 2007; Drummond et al., 2012). All other parameters and the  
258 Markov-chain Monte Carlo settings were left at the default settings. The xml input files for both the  
259 lognormal and normal distribution analyses are available through Penn State's ScholarSphere repository  
260 (DOI: 10.18113/S1D06H).

261 **RESULTS AND DISCUSSION**262 **Phylogenetic analyses**

263 The final concatenated data set consisted of 3097 characters total: *COI* (681bp), *16S* (371bp, excluding  
264 RAAs), *28S* (428bp, excluding RAAs), *AM2* (672bp), *CAD1* (417bp, excluding the intron), *CAD2* (321bp),  
265 and *RPS23* (207bp, excluding the intron). Individual gene trees are depicted in Supplementary Figures  
266 S1-S7. The null hypothesis for base composition homogeneity was rejected for *AM2* ( $\chi^2 = 368.819$ ,  
267  $df = 120$ ;  $P = 0.000000000$ ) and *COI* ( $\chi^2 = 562.535$ ,  $P = 0.0000000$ ) (Table S3). Average nucleotide  
268 composition across all genes and gene regions analyzed are depicted in Table S3.

269 The Bayesian analysis of the concatenated dataset recovered a well resolved tree with most clades  
270 well supported ( $pp > 0.95$ ) (Figure 2). Clades recovered across the individual gene trees and for the  
271 concatenated analysis are summarized in Table S4 and gene trees are depicted in Figures S1-S7. We  
272 also performed a Maximum Likelihood analysis with RaxML v8.2.4 (Stamatakis, 2014, 2006) (Figure  
273 S15) under the GTR+CAT model and auto-determination of bootstrap replicates. The phylogenies  
274 obtained from BEAST (Figure 3), Mr.Bayes (Figure 2), and RaxML (Figure S15) were very similar except  
275 relationships among species varied within genera and *Micrevania* was not monophyletic in the Bayesian  
276 analysis (Figure 2). The placement of *Rothevania* also varied across analyses.

277 In the concatenated analysis (Figure 2), Evaniidae was recovered as monophyletic with high support  
278 ( $pp = 1.0$ ). Of the 15 genera included in the analysis with more than one representative, nine were  
279 recovered as monophyletic, including *Evaniscus*, *Decevania*, *Semaeomyia*, *Evania*, *Hyptia*, *Brachygaster*,  
280 *Prosevania*, *Trissevania*, and *Evaniella*. All clades representing monophyletic genera had posterior  
281 probabilities of 1.0. Although *Micrevania* was recovered as paraphyletic, it was recovered as monophyletic  
282 in other analyses, as mentioned above, the divergence analysis (Figure 3), ML analysis (Fig S.15) and  
283 the *16S* and *COI* individual gene analyses (Table S3) and previously by Deans et al. (2006).

284 Similar to the previous study (Deans et al., 2006), *Parevania* and *Zeuxevania* were recovered as  
285 paraphyletic with respect to each other, but in a well-supported clade ( $pp = 1.0$ ) with *Papatuka*, in the  
286 concatenated analysis as well as five of the seven gene trees (Table S4). Interestingly, all of these taxa  
287 have a distinct sequence motif at the 3' end of the *RPS23* intron: GTTTGTTTTGYAG (Fig. S9). No other  
288 evaniid taxa have a similar motif at the 3' end (Fig. S8), and thus the motif is diagnostic for this clade.  
289 *Trissevania* and *Evania* were recovered as sister taxa with high support ( $pp = 1.0$ ) in the concatenated  
290 analysis and these two taxa were recovered as sister to *Zeuxevania + Parevania + Papatuka* ( $pp = 0.98$ )  
291 (Figure 2). But there was little support for these higher level relationships among in the individual gene  
292 trees (Table S4). *Brachygaster* was recovered as sister to *Prosevania* with strong support ( $pp = 1.0$ ) but  
293 was only recovered in the *CAD2* gene tree (Fig. S4). *Micrevania* was also recovered as the sister to  
294 all remaining evaniids, followed by *Brachygaster + Prosevania* in the concatenated analysis. Yet, the  
295 position of these taxa fluctuated widely among the individual gene trees, likely due to inconsistent taxon  
296 sampling across the gene trees.

297 *Acanthinevania* and *Szepligetella* were consistently recovered together ( $pp = 1.0$  in the concatenated  
298 analysis (Figure 2) and all gene trees except *16S* (Table S4), but were paraphyletic with respect to  
299 each other. Interestingly, all members of *Acanthinevania* and *Szepligetella* have a GATCTAAC motif  
300 (Fig. S10) in the *RPS23* intron that is not shared with any other evaniid taxa (Fig. S8), highlighting  
301 their close evolutionary relationship. There are also two diagnostic motifs within regions of ambiguous  
302 alignment (RAAs) that were excluded from the phylogenetic analyses. All members of *Acanthinevania* and  
303 *Szepligetella* have the motif TAAAAT in RAA8 (Fig. S11) and the motif TGCAAT within RAA12 (Fig.  
304 S12). *Evaniella* was recovered as the sister group to *Acanthinevania + Szepligetella* in the concatenated  
305 analysis and in three genes trees (Table S4). Members of all three genera share a 9bp diagnostic motif in  
306 RAA10 in *28S*: YTCGAWAAA (Fig. S12). Most other evaniid taxa do not have this many base pairs in  
307 this position (usually 2–4bp); the ones that do have longer motifs are radically different in sequence (the  
308 full alignment is available in Scholarsphere, DOI:10.18113/S1D06H). *Alobevania* was recovered as sister  
309 to *Evaniella + (Acanthinevania + Szepligetella)*, with strong support in the concatenated analysis, and  
310 with moderate support ( $pp = 0.88$ ) in the *28S* gene tree. This result is unsurprising given that these taxa  
311 were once treated as *Evaniella* (Deans and Huben, 2003).

312 New world taxa with reduced wing venation (*Evaniscus*, *Decevania*, *Hyptia*, *Rothevania*, and *Se-*  
313 *maeomyia*) are recovered together in a well-supported clade ( $pp = 1.0$ ), in the concatenated analysis  
314 (Figure 2). This clade is only recovered in the *CAD1* gene tree (Figure S4), possibly due to lower taxo-  
315 nomic sampling in some individual gene trees due to failed amplification. However, these taxa are present

316 in various combinations throughout the individual gene trees, but the relationships among taxa fluctuate  
 317 widely, which is also reflected in the lower support values in the concatenated tree for relationships among  
 318 these genera (Figure 2).

### 319 Divergence time analyses

320 The phylogenies obtained from the two Bayesian uncorrelated relaxed clock analyses using BEAST were  
 321 both identical (Figure 3 (simplified chronogram from the log-normal distribution) and Fig S14 (normal  
 322 distribution)). Other than slight differences among species within genera, and the recovery of *Micreвания*  
 323 as monophyletic, the trees were very similar to the tree obtained from the analysis with MrBayes (Figure  
 324 2). Estimates of divergence time from both analyses, using either a log-normal and normal distribution  
 325 are listed in Table 2. The log-normal analysis estimated younger divergence times for all clades (Table  
 326 2). This was expected as the calibration bounds were constrained within 25 million years of the fossil's  
 327 age in the log-normal analysis, but were allowed to vary across a larger span of time in the normal  
 328 distribution analysis based on interpretations of the fossil record. It is likely that the normal analysis  
 329 uses too broad a range, with the maximum bound being set too far away from the oldest known fossil  
 330 for the crown lineage, and thus we depict the log-normal analysis (Figure 3) and use these dates to draw  
 331 inferences about evaniid clade divergence. Evaniidae was estimated to diverge around 137 million years  
 332 ago (Mya) (134.1–141.1). Although the superfamily was not the focus of this study, Evanioidea had  
 333 an estimated mean age of 168 Mya (135.9–199.0), consistent with other previous estimates suggesting  
 334 Evanioidea diverged in the mid-late Jurassic (Peters et al., 2017; Branstetter et al., 2017). Branches  
 335 leading to *Micreвания*, *Proseвания*, and *Brachygaster* split sometime around the end of the Cretaceous,  
 336 with means ranging between 60–73 Mya (Table 2). Other extant genera likely diverged sometime in the  
 337 early Cenozoic and these lineages were likely all present before the start of the Neogene (Figure 3, Table  
 338 2).

	Log-normal - Age (My) mean (95% HDP)	Normal - Age (My) mean (95% HDP)
<i>Gasteruption</i> (Gasteruptionidae)	38.6 (18.5–59.3)	46.3 (27.2–69.4)
<i>Pristaulacus</i> (Aulacidae)	49.1 (45.4–54.7)	48.9 (23.3–73.6)
<b>Evaniidae</b>	<b>136.8 (134.1–141.4)</b>	<b>151.5 (135.9–166.7)</b>
<i>Brachygaster</i>	60.7 (40.5–86.4)	72.1 (49.5–96.3)
<i>Deceвания</i>	37.6 (25.2–51.1)	47.8 (31.6–64.0)
<i>Eвания</i>	45.3 (33.3–58.6)	55.4 (40.5–70.7)
<i>Evaniella</i>	69.3 (55.5–84.0)	88.6 (73.5–104.3)
<i>Evaniscus</i>	66.0 (40.8–89.5)	80.4 (50.1–110.3)
<i>Hyptia</i>	50.7 (45.7–57.8)	65.4 (50.7–81.2)
<i>Micreвания</i>	67.8 (38.4–94.8)	80.1 (52.5–111.8)
<i>Proseвания</i>	72.1 (58.6–86.4)	85.7 (67.6–103.8)
<i>Semaemyia</i>	59.0 (46.6–72.5)	76.9 (61.1–94.0)
<i>Szeplitella s.l.</i>	49.0 (38.3–60.1)	60.6 (48.6–72.1)
<i>Trisseвания</i>	32.0 (17.5–50.4)	38.5 (20.5–57.3)
<i>Zeuxevania s.l.</i>	55.6 (45.8–66.3)	76.0 (59.6–92.2)

**Table 2.** Estimates of divergence times for Evaniidae (bolded) and outgroups based on an uncorrelated log-normal relaxed clock analyses. Six fossil calibrations were used (see Supplementary Material) with maximum bounds for clade ages set using a log-normal (Analysis 1) and normal distribution (Analysis 2). For each analysis the mean age in millions of years (My) and the 95% highest posterior density interval (HDP, equivalent to a confidence interval) is provided.

### 339 Novel genes and molecular signatures

340 *Alpha-mannosidase 2* (*AM2*) has never been used before in phylogenetic studies. This gene has a mix of  
 341 conserved and variable sites (44% parsimony-informative sites), but it failed the test for base composition  
 342 homogeneity, which can cause systematic biases in phylogenetic analyses (Phillips et al., 2004; Rodríguez-  
 343 Ezpeleta et al., 2007; Sharanowski et al., 2011). RY-coding this gene did not change the results obtained

344 from the concatenated analysis. Unfortunately amplification of *AM2* was difficult, even with the addition  
 345 of PCR additives such as DMSO, causing a high amount of missing data. Gel cuts were often necessary  
 346 to achieve clean sequences for several genes, but particularly *AM2*. *RPS23* was highly conserved in the  
 347 exonic regions, and thus may be better suited for deeper level studies across families. There were distinct  
 348 molecular signatures within the intronic region that would be very useful for lower level studies, such as  
 349 across species, or population-level studies (see Lohse et al., 2010). The molecular motifs in the *RPS23*  
 350 intron were useful for delimiting genera and diagnosing congenics (see taxonomic implications, below).  
 351 The individual gene trees for both regions of *CAD* were relatively well resolved (Figures S4-5) and similar  
 352 to other studies (Desjardins et al., 2007; Sharanowski et al., 2011), which demonstrates good utility for  
 353 resolving phylogenetic relationships in Hymenoptera.

354 Alignments based on secondary structure for rDNA have been very useful for delimiting highly  
 355 variable regions to exclude from analyses to achieve better phylogenetic results (Gillespie et al., 2005b;  
 356 Pitz et al., 2007). However, variable regions have useful information with phylogenetic and taxonomic  
 357 utility, as demonstrated by Sharanowski et al. (2011), who included variable regions (RECs, RAAs, and  
 358 RSCs) if the variation in sequence length had a standard deviation less than one. Here we demonstrate the  
 359 utility of some of these regions for diagnosing genera (Figures S11-12) and use these data to improve  
 360 taxonomic classifications (see Taxonomic implications below).

### 361 Taxonomic implications

362 Relative to the Deans et al. (2006) study, the addition of several more genes and taxa clearly led to  
 363 increased resolution. For example, an additional four genera were recovered as monophyletic, and higher  
 364 level relationships were more resolved and better supported. Our understanding of evaniid relationships  
 365 remains incomplete, but, based on mounting evidence here and through our observations of morphology,  
 366 we feel comfortable proposing the following classificatory changes.

367 **New synonyms of *Zeuxevania* and new combinations** *Parevania*, **syn. nov.**, and *Papatuka*, **syn.**  
 368 **nov.**, are congeneric with and junior synonyms of *Zeuxevania*. Bradley (1908) also suspected that these  
 369 two taxa were congeneric and treated *Parevania* as a subgenus of *Zeuxevania*. These taxa are consistently  
 370 recovered together in well-supported clades across individual gene trees and within the concatenated  
 371 analyses, but are polyphyletic with respect to each other (Table S4). Additionally, there are molecular  
 372 signatures within the *RPS23* intron that support their shared evolutionary history (Fig. S9). ARD has  
 373 observed thousands of specimens of these taxa and can find no consistency in the presence or absence of  
 374 the fore wing vein 1RS, which was the only character purported to separate *Parevania* and *Zeuxevania*  
 375 (Deans and Huben, 2003).

376 Following the taxonomy of Hedicke (1939), we hereby transfer the following species back to *Zeuxe-*  
 377 *vania*: *albitarsus* (Cameron, 1899); *annulicornis* (Turner, 1927); *atra* (Kieffer, 1916); *bisulcata* (Kieffer,  
 378 1911); *curvicarinata* (Cameron, 1899); *kriegeriana* (Enderlein, 1905); *leucostoma* (Kieffer, 1910); *longi-*  
 379 *calcar* (Kieffer, 1911); *punctatissima* (Kieffer, 1911); *rubra* (Cameron, 1905); *sanguineiceps* (Turner,  
 380 1927); *schlettereri* Bradley 1908; *schoenlandi* (Cameron, 1905); *semirufa* (Kieffer, 1907).

381 We also transfer the following species to *Zeuxevania* for the first time: *aurata* (Benoit, 1950), **comb.**  
 382 **nov.**; *brevis* (Brues, 1933), **comb. nov.**; *broomi* (Cameron, 1906), **comb. nov.**; *emarginata* (Kieffer,  
 383 1911), **comb. nov.**; *kasauliensis* (Muzaffer, 1943), **comb. nov.**; *laeviceps* (Enderlein, 1913), **comb. nov.**;  
 384 *madegassa* (Benoit, 1952), **comb. nov.**; *meridionalis* (Cameron, 1906), **comb. nov.**; *micholitzii* (Enderlein,  
 385 1905), **comb. nov.**; *ortegae* (Ceballos, 1966), **comb. nov.**; *plana* (Benoit, 1952), **comb. nov.**; *producta*  
 386 (Brues, 1933), **comb. nov.**; *remanea* (Brues, 1933), **comb. nov.**.

387 *Papatuka* was originally described from a single, apterous specimen (Deans, 2002) and was since  
 388 expanded to include other, winged species (Deans, 2005). The morphology of these species, which is  
 389 also reflected in the molecular data, is not substantially different from *Zeuxevania*, and we transfer those  
 390 species to *Zeuxevania*: *alamunyiga* (Deans, 2002), **comb. nov.**; *capensis* (Schletterer, 1886), **comb. nov.**;  
 391 *longitarsis* (Kieffer, 1904), **comb. nov.**

392 **New synonym of *Szepligetella* and new combinations** There is also abundant evidence to support  
 393 *Acanthinevania* as congeneric with *Szepligetella*. They are consistently recovered together in a clade but  
 394 neither appears to be monophyletic by itself (Table S4). The primary diagnostic characters that separated  
 395 these two primarily Australian genera include: *Szepligetella* with the third labial palpomere swollen;  
 396 *Acanthinevania* with an elongated head relative to *Szepligetella*; and *Acanthinevania* with labium folded

397 strongly anteriorly and thus appearing long and narrow, not broad and flat as in most *Szepligetella* (Deans  
398 and Huben, 2003). Our observations of more than 1,000 specimens reveal that these character states (e.g.,  
399 face long vs. face short) fall along phenotypic gradients, with no discrete sets of states. Several molecular  
400 characters link (but do not separate) these genera, including motifs present in the *RPS23* intron and at  
401 least two regions of 28S (Figs S10-12).

402 We treat *Acanthinevania*, **syn. nov.**, as *Szepligetella* and transfer the following species to *Szepligetella*:  
403 *australis* (Schletterer, 1886), **comb. nov.**; *braunsi* (Kieffer, 1911), **comb. nov.**; *braunsiana* (Kieffer,  
404 1911), **comb. nov.**; *clavaticornis* (Kieffer, 1911), **comb. nov.**; *erythrogaster* (Kieffer, 1904), **comb. nov.**;  
405 *eximia* (Schletterer, 1886), **comb. nov.**; *genalis* (Schletterer, 1886), **comb. nov.**; *humerala* (Schletterer,  
406 1889), **comb. nov.**; *leucocras* (Kieffer, 1911), **comb. nov.**; *longigena* (Schletterer, 1889), **comb. nov.**;  
407 *lucida* (Schletterer, 1889), **comb. nov.**; *mediana* (Schletterer, 1889), **comb. nov.**; *princeps* (Westwood,  
408 1841), **comb. nov.**; *quinclineata* (Kieffer, 1904), **comb. nov.**; *rufiventris* (Kieffer, 1911), **comb. nov.**;  
409 *scabra* (Schletterer, 1889), **comb. nov.**; *sericans* (Westwood, 1851), **comb. nov.**; *striatifrons* (Kieffer,  
410 1904), **comb. nov.**; *szepligeti* (Bradley, 1908), **comb. nov.**; *versicolor* (Kieffer, 1904), **comb. nov.**;  
411 *villosicrus* (Kieffer, 1904), **comb. nov.**

412 **Emerging tribal classification** A new tribal classification for Evaniidae is warranted, given the lack of  
413 support for Bradley's (1908) original (>100 year-old) tribal concepts (Deans, 2005; Deans et al., 2006;  
414 Deans and Huben, 2003). Mikó et al. (2014) recently described Trissevaniini, to include *Trissevania* and  
415 *Afrevania*, and, based on our results here, molecular work by (Deans et al., 2006), and prior morphological  
416 work by us and our colleagues (Deans and Huben, 2003; Deans and Kawada, 2008; Kawada and Azevedo,  
417 2007; Kawada, 2011) we have an opportunity to revise Hyptiini to include those New World genera  
418 with reduced wing venation: *Evaniscus*, *Hyptia*, *Rothevania*, *Semaeomyia*, and *Decevania*. We remove  
419 *Brachygaster*, *Evaniella*, and *Zeuxevania* from Hyptiini (see Bradley, 1908). This updated concept of  
420 Hyptiini can be separated from other evaniid taxa by the absence of at least the fore wing RS+M, and  
421 usually many other apical veins (see Figs. 1, 9, 11, 16, 17 in Deans and Huben, 2003), and its origin in  
422 the New World.

### 423 **Evaniid divergence and evolution**

424 Evaniids diverged in the Early Cretaceous (ca. 134.1–141.1 Mya), when numerous modern cockroach  
425 fossils have been found (Grimaldi and Engel, 2005), although cockroaches with oothecae are thought  
426 to have much earlier origins in the Late Carboniferous (Legendre et al., 2015). Most of the extant  
427 evaniid genera diverged sometime near the K-T boundary, which may indicate that the mass extinction  
428 played a role in the divergence of multiple new lineages of ensign wasps. Whether or not there has been  
429 co-cladogenesis with modern cockroach lineages remains to be tested but would be hampered by the lack  
430 of known host relationships for most evaniids (Deans, 2005). For evaniids, as for most Hymenoptera,  
431 basic natural history research is needed to understand the trophic relationships among wasps and their  
432 hosts.

### 433 **CONCLUSION**

434 We provide here a more robust and well-resolved phylogeny for Evaniidae than previous studies, which  
435 will facilitate ongoing evolutionary and taxonomic work. Indeed, the new synonyms and combinations  
436 proposed above help us progress towards a stable classification that reflects evolutionary relationships.  
437 Building on prior results (Deans et al., 2006), our data also reveal new, useful markers for Hymenoptera  
438 (*AM2* and *RPS23*) and continue to support the utility of shared molecular motifs in defining major clades  
439 in Evaniidae. Our results indicate that Evaniidae diverged in the early Cretaceous with most genera  
440 diversifying in the late Cretaceous or early Tertiary. The results also highlight important targets for future  
441 data collection, especially near the base of the tree (*Micrevania*) and the relationships within each genus.  
442 More intensive sampling, especially with the addition of morphological data and fossils (e.g., Ronquist  
443 et al., 2012a), is the logical next step in providing a tribal classification and more refined estimates for  
444 divergence times.

### 445 **ACKNOWLEDGMENTS**

446 We are grateful to Mike Irwin, Martin Hauser, Kevin Holston, Jack Longino, Mike Sharkey, the late Evert  
447 Schlinger, the late Don Webb, and countless other collectors who shared material with us. We also thank

448 the numerous loan facilitators, without whom this work would be impossible and the three reviewers who  
449 helped improved the manuscript.

## 450 REFERENCES

- 451 Aleshin, V., Mikhailov, K., Konstantinova, A., Nikitin, M., Rusin, L. Y., Buinova, D., Kedrova, O., and  
452 Petrov, N. (2009). On the phylogenetic position of insects in the Pancrustacea clade. *Molecular Biology*,  
453 43(5):804–818.
- 454 Altschul, S. F., Gish, W., Miller, W., Myers, E. W., and Lipman, D. J. (1990). Basic local alignment  
455 search tool. *Journal of molecular biology*, 215(3):403–410.
- 456 Balhoff, J. P., Mikó, I., Yoder, M. J., Mullins, P. L., and Deans, A. R. (2013). A semantic model for species  
457 description applied to the ensign wasps (Hymenoptera: Evaniidae) of New Caledonia. *Systematic  
458 Biology*, 62(5):639–659.
- 459 Bradley, J. C. (1908). The Evaniidæ, ensign-flies, an archiac family of Hymenoptera. *Transactions of the  
460 American Entomological Society*, 34(2):101–194.
- 461 Branstetter, M. G., Danforth, B. N., Pitts, J. P., Faircloth, B. C., Ward, P. S., Buffington, M. L., Gates,  
462 M. W., Kula, R. R., and Brady, S. G. (2017). Phylogenomic insights into the evolution of stinging  
463 wasps and the origins of ants and bees. *Current Biology*, 27(7):1019–1025.
- 464 Brues, C. T. (1933). The parasitic Hymenoptera of the Baltic amber. part 1. *Bernstein-Forschungen*,  
465 3:4–172.
- 466 Cardinal, S. and Danforth, B. N. (2013). Bees diversified in the age of eudicots. *Proceedings of the Royal  
467 Society of London B: Biological Sciences*, 280(1755).
- 468 Danforth, B. N., Fang, J., and Sipes, S. (2006). Analysis of family-level relationships in bees (Hy-  
469 menoptera: Apiformes) using 28S and two previously unexplored nuclear genes: CAD and RNA  
470 polymerase II. *Molecular Phylogenetics and Evolution*, 39(2):358–372.
- 471 Deans, A. and Huben, M. (2003). Annotated key to the ensign wasp (Hymenoptera: Evaniidae) genera  
472 of the world, with descriptions of three new genera. *Proceedings of the Entomological Society of  
473 Washington*, 105:859–875.
- 474 Deans, A. R. (2002). *Papatuka alamunyiga* Deans, a new genus and species of apterous ensign wasp  
475 (Hymenoptera: Evaniidae) from Kenya. *Zootaxa*, 95(1):1–8.
- 476 Deans, A. R. (2005). *Annotated catalog of the world's ensign wasp species (Hymenoptera: Evaniidae)*,  
477 volume 34. American Entomological Institute.
- 478 Deans, A. R., Basibuyuk, H. H., Azar, D., and Nel, A. (2004). Descriptions of two new Early Cretaceous  
479 (Hauterivian) ensign wasp genera (Hymenoptera: Evaniidae) from lebanese amber. *Cretaceous  
480 Research*, 25(4):509–516.
- 481 Deans, A. R., Gillespie, J. J., and Yoder, M. J. (2006). An evaluation of ensign wasp classification  
482 (Hymenoptera: Evaniidae) based on molecular data and insights from ribosomal RNA secondary  
483 structure. *Systematic Entomology*, 31(3):517–528.
- 484 Deans, A. R. and Kawada, R. (2008). *Alobevania*, a new genus of neotropical ensign wasps (Hymenoptera:  
485 Evaniidae), with three new species: integrating taxonomy with the World Wide Web. *Zootaxa*, 1787:28–  
486 44.
- 487 Desjardins, C. A., Regier, J. C., and Mitter, C. (2007). Phylogeny of pteromalid parasitic wasps (Hy-  
488 menoptera: Pteromalidae): initial evidence from four protein-coding nuclear genes. *Molecular  
489 Phylogenetics and Evolution*, 45(2):454–469.
- 490 Downton, M. and Austin, A. D. (1994). Molecular phylogeny of the insect order Hymenoptera: Apocritan  
491 relationships. *Proceedings of the National Academy of Sciences USA*, 91(21):9911–9915.
- 492 Downton, M. and Austin, A. D. (2001). Simultaneous analysis of 16S, 28S, COI and morphology in the  
493 Hymenoptera: Apocrita—evolutionary transitions among parasitic wasps. *Biological Journal of the  
494 Linnean Society*, 74(1):87–111.
- 495 Drummond, A. J., Nicholls, G. K., Rodrigo, A. G., and Solomon, W. (2002). Estimating mutation  
496 parameters, population history and genealogy simultaneously from temporally spaced sequence data.  
497 *Genetics*, 161(3):1307–1320.
- 498 Drummond, A. J. and Rambaut, A. (2007). BEAST: Bayesian evolutionary analysis by sampling trees.  
499 *BMC evolutionary biology*, 7(1):214.
- 500 Drummond, A. J., Suchard, M. A., Xie, D., and Rambaut, A. (2012). Bayesian phylogenetics with  
501 BEAUti and the BEAST 1.7. *Molecular biology and evolution*, 29(8):1969–1973.

- 502 Folmer, O., Black, M., Hoeh, W., Lutz, R., and Vrijenhoek, R. (1994). DNA primers for amplification of  
503 mitochondrial cytochrome c oxidase subunit I from diverse metazoan invertebrates. *Molecular marine*  
504 *biology and biotechnology*, 3(5):294–299.
- 505 Gillespie, J. J., Munro, J. B., Heraty, J. M., Yoder, M. J., Owen, A. K., and Carmichael, A. E. (2005a).  
506 A secondary structural model of the 28S rRNA expansion segments D2 and D3 for chalcidoid wasps  
507 (Hymenoptera: Chalcidoidea). *Molecular Biology and Evolution*, 22(7):1593–1608.
- 508 Gillespie, J. J., Yoder, M. J., and Wharton, R. A. (2005b). Predicted secondary structure for 28S and 18S  
509 rRNA from Ichneumonoidea (Insecta: Hymenoptera: Apocrita): impact on sequence alignment and  
510 phylogeny estimation. *Journal of Molecular Evolution*, 61(1):114–137.
- 511 Gonzalez, D. S. and Jordan, I. K. (2000). The  $\alpha$ -mannosidases: phylogeny and adaptive diversification.  
512 *Molecular Biology and Evolution*, 17(2):292–300.
- 513 Grimaldi, D. and Engel, M. S. (2005). *Evolution of the Insects*. Cambridge University Press.
- 514 Hall, T. A. (1999). BioEdit: a user-friendly biological sequence alignment editor and analysis program  
515 for Windows 95/98/NT. In *Nucleic acids symposium series*, volume 41, pages 95–98. [London]:  
516 Information Retrieval Ltd., c1979-c2000.
- 517 Hasegawa, M., Kishino, H., and Yano, T.-a. (1985). Dating of the human-ape splitting by a molecular  
518 clock of mitochondrial dna. *Journal of molecular evolution*, 22(2):160–174.
- 519 Hedicke, H. (1939). Evaniidae. In Hedicke, H., editor, *Hymenopterum Catalogus Pars 9*. Dr. W. Junk,  
520 Gravenhage.
- 521 Huben, M. (1995). Evaniidae. In Hanson, P. and Gauld, I., editors, *The Hymenoptera of Costa Rica*,  
522 pages 195–199. Oxford University Press.
- 523 Jennings, J. T., Austin, A. D., and Stevens, N. B. (2004). *Hyptiogastrites electrinus* Cockerell, 1917,  
524 from Myanmar (Burmese) amber: redescription and its placement within the Evanioidea (Insecta:  
525 Hymenoptera). *Journal of Systematic Palaeontology*, 2(2):127–132.
- 526 Jennings, J. T. and Krogmann, L. (2009). A new species of *Pristaulacus* kieffer (Hymenoptera: Aulacidae)  
527 from Baltic amber. *Insect Systematics & Evolution*, 40(2):201–207.
- 528 Jennings, J. T., Krogmann, L., and Mew, S. L. (2012). *Hyptia deansi* sp. nov., the first record of Evaniidae  
529 (Hymenoptera) from Mexican amber. *Zootaxa*, 3349(1):63–68.
- 530 Jennings, J. T., Krogmann, L., and Priya, P. (2013). Happy birthday Willi Hennig!—*Hyptia hennigi* sp. nov.  
531 (Hymenoptera: Evaniidae), a fossil ensign wasp from Eocene Baltic amber. *Zootaxa*, 3731:395–398.
- 532 Katoh, K. and Standley, D. M. (2013). MAFFT multiple sequence alignment software version 7:  
533 improvements in performance and usability. *Molecular biology and evolution*, 30(4):772–780.
- 534 Kawada, R. (2011). Pictorial key for females of *Decevania* Huben (Hymenoptera, Evaniidae) and  
535 description of a new species. *ZooKeys*, (116):59–84.
- 536 Kawada, R. and Azevedo, C. (2007). Taxonomic revision of the neotropical ensign wasp genus *Decevania*  
537 (Hymenoptera: Evaniidae). *Zootaxa*, 1496(1):1–30.
- 538 Lanfear, R., Calcott, B., Ho, S. Y., and Guindon, S. (2012). PartitionFinder: combined selection of  
539 partitioning schemes and substitution models for phylogenetic analyses. *Molecular biology and*  
540 *evolution*, 29(6):1695–1701.
- 541 Legendre, F., Nel, A., Svenson, G. J., Robillard, T., Pellens, R., and Grandcolas, P. (2015). Phylogeny of  
542 Dictyoptera: dating the origin of cockroaches, praying mantises and termites with molecular data and  
543 controlled fossil evidence. *Plos ONE*, 10(7):e0130127.
- 544 Li, L., Rasnitsyn, A. P., Shih, C., Labandeira, C. C., Buffington, M., Li, D., and Ren, D. (2018). Phylogeny  
545 of Evanioidea (Hymenoptera, Apocrita), with descriptions of new Mesozoic species from China and  
546 Myanmar. *Systematic Entomology*, 43(4):810–842.
- 547 Li, W., Cowley, A., Uludag, M., Gur, T., McWilliam, H., Squizzato, S., Park, Y. M., Buso, N., and  
548 Lopez, R. (2015). The embl-ebi bioinformatics web and programmatic tools framework. *Nucleic acids*  
549 *research*, 43(W1):W580–W584.
- 550 Lohse, K., Sharanowski, B., Blaxter, M., Nicholls, J. A., and Stone, G. N. (2011). Developing EPIC  
551 markers for chalcidoid hymenoptera from EST and genomic data. *Molecular ecology resources*,  
552 11(3):521–529.
- 553 Lohse, K., Sharanowski, B., and Stone, G. N. (2010). Quantifying the Pleistocene history of the oak gall  
554 parasitoid *Cecidostiba fungosa* using twenty intron loci. *Evolution*, 64(9):2664–2681.
- 555 Marchler-Bauer, A., Derbyshire, M. K., Gonzales, N. R., Lu, S., Chitsaz, F., Geer, L. Y., Geer, R. C., He,  
556 J., Gwadz, M., Hurwitz, D. I., Lanczycki, C. J., Lu, F., Marchler, G. H., Song, J. S., Thanki, N., Wang,

- 557 Z., Yamashita, R. A., Zhang, D., Zheng, C., and Bryant, S. H. (2015). CDD: NCBI's conserved domain  
558 database. *Nucleic Acids Research*, 43(D1):D222–D226.
- 559 Mardulyn, P. and Whitfield, J. B. (1999). Phylogenetic signal in the *coi*, 16s, and 28s genes for infer-  
560 ring relationships among genera of Microgastrinae (Hymenoptera; Braconidae): evidence of a high  
561 diversification rate in this group of parasitoids. *Molecular Phylogenetics and Evolution*, 12(3):282–294.
- 562 Mikó, I., Copeland, R. S., Balhoff, J. P., Yoder, M. J., and Deans, A. R. (2014). Folding wings like a  
563 cockroach: a review of transverse wing folding ensign wasps (Hymenoptera: Evaniidae: *Afrevania* and  
564 *Trissevania*). *PLoS ONE*, 9(5):e94056.
- 565 Miller, M. A., Pfeiffer, W., and Schwartz, T. (2010). Creating the CIPRES Science Gateway for inference  
566 of large phylogenetic trees. In *Gateway Computing Environments Workshop (GCE), 2010*, pages 1–8.  
567 IEEE.
- 568 Moulton, J. K. and Wiegmann, B. M. (2004). Evolution and phylogenetic utility of CAD (rudimen-  
569 tary) among mesozoic-aged eremoneuran Diptera (Insecta). *Molecular phylogenetics and evolution*,  
570 31(1):363–378.
- 571 Namin, H. H., Iranpour, M., and Sharanowski, B. J. (2014). Phylogenetics and molecular identification of  
572 the *Ochlerotatus communis* complex (Diptera: Culicidae) using DNA barcoding and polymerase chain  
573 reaction-restriction fragment length polymorphism. *The Canadian Entomologist*, 146(1):26–35.
- 574 Nel, A., Martínez-Delclòs, X., and Azar, D. (2002). A new ensign-fly from the Lower-Middle Miocene Do-  
575 minican amber (Hymenoptera, Evaniidae). *Bulletin de la Société entomologique de France*, 107(3):217–  
576 221.
- 577 Peters, R. S., Krogmann, L., Mayer, C., Donath, A., Gunkel, S., Meusemann, K., Kozlov, A., Podsiad-  
578 lowski, L., Petersen, M., Lanfear, R., Diez, P. A., Heraty, J., Kjer, K. M., Klopstein, S., Meier, R.,  
579 Polidori, C., Schmitt, T., Liu, S., Zhou, X., Wappler, T., Rust, J., Misof, B., and Niehuis, O. (2017).  
580 Evolutionary history of the Hymenoptera. *Current Biology*, 27(7):1013–1018.
- 581 Peñalver, E., Ortega-Blanco, J., Nel, A., and Delclòs, X. (2010). Mesozoic Evaniidae (Insecta: Hy-  
582 menoptera) in Spanish amber: Reanalysis of the phylogeny of the Evanioidea. *Acta Geologica Sinica*  
583 (*English Edition*), 84(4):809–827.
- 584 Phillips, M. J., Delsuc, F., and Penny, D. (2004). Genome-scale phylogeny and the detection of systematic  
585 biases. *Molecular biology and evolution*, 21(7):1455–1458.
- 586 Pitz, K. M., Dowling, A. P., Sharanowski, B. J., Boring, C. A., Seltmann, K. C., and Sharkey, M. J. (2007).  
587 Phylogenetic relationships among the Braconidae (Hymenoptera: Ichneumonoidea): A reassessment of  
588 Shi, Chen, and van Achterberg (2005). *Molecular Phylogenetics and Evolution*, 43(1):338–343.
- 589 Rambaut, A. (2012). FigTree v. 1. 4. *Molecular evolution, phylogenetics and epidemiology*. Edinburgh,  
590 UK: University of Edinburgh, Institute of Evolutionary Biology.
- 591 Rambaut, A. and Drummond, A. (2009). Tracer v1.5. Available at [http://tree.bio.ed.ac.uk/  
592 software/tracer/](http://tree.bio.ed.ac.uk/software/tracer/) Accessed 19 February 2018.
- 593 Rasnitsyn, A. P., Jarzembowski, E. A., and Ross, A. J. (1998). Wasps (Insecta: Vespida = Hymenoptera)  
594 from the Purbeck and Wealden (Lower Cretaceous) of southern England and their biostratigraphical  
595 and palaeoenvironmental significance. *Cretaceous Research*, 19(3-4):329–391.
- 596 Rodríguez-Ezpeleta, N., Brinkmann, H., Roure, B., Lartillot, N., Lang, B. F., and Philippe, H. (2007). De-  
597 tecting and overcoming systematic errors in genome-scale phylogenies. *Systematic Biology*, 56(3):389–  
598 399.
- 599 Ronquist, F., Klopstein, S., Vilhelmsen, L., Schulmeister, S., Murray, D. L., and Rasnitsyn, A. P. (2012a).  
600 A total-evidence approach to dating with fossils, applied to the early radiation of the Hymenoptera.  
601 *Systematic Biology*, 61(6):973–999.
- 602 Ronquist, F., Teslenko, M., Van Der Mark, P., Ayres, D. L., Darling, A., Höhna, S., Larget, B., Liu,  
603 L., Suchard, M. A., and Huelsenbeck, J. P. (2012b). MrBayes 3.2: efficient Bayesian phylogenetic  
604 inference and model choice across a large model space. *Systematic Biology*, 61(3):539–542.
- 605 Sawoniewicz, J. and Kupryjanowicz, J. (2003). *Evaniella eocenica* sp. nov. from the Baltic amber  
606 (Hymenoptera: Evaniidae). *Acta Zoologica Cracoviensia*, 46(Suppl. - Fossil Insects):267–270.
- 607 Schulmeister, S., Wheeler, W. C., and Carpenter, J. M. (2002). Simultaneous analysis of the basal lineages  
608 of Hymenoptera (Insecta) using sensitivity analysis. *Cladistics*, 18(5):455–484.
- 609 Sharanowski, B. J., Dowling, A. P., and Sharkey, M. J. (2011). Molecular phylogenetics of Braconidae  
610 (Hymenoptera: Ichneumonoidea), based on multiple nuclear genes, and implications for classification.  
611 *Systematic Entomology*, 36(3):549–572.



- 612 Sharanowski, B. J., Robbertse, B., Walker, J., Voss, S. R., Yoder, R., Spatafora, J., and Sharkey, M. J.  
613 (2010). Expressed sequence tags reveal Proctotrupomorpha (minus Chalcidoidea) as sister to Aculeata  
614 (Hymenoptera: Insecta). *Molecular phylogenetics and evolution*, 57(1):101–112.
- 615 Stadler, T. (2009). On incomplete sampling under birth-death models and connections to the sampling-  
616 based coalescent. *Journal of theoretical biology*, 261(1):58–66.
- 617 Stamatakis, A. (2006). RAxML-VI-HPC: maximum likelihood-based phylogenetic analyses with thou-  
618 sands of taxa and mixed models. *Bioinformatics*, 22(21):2688–2690.
- 619 Stamatakis, A. (2014). Raxml version 8: a tool for phylogenetic analysis and post-analysis of large  
620 phylogenies. *Bioinformatics*, 30(9):1312–1313.
- 621 Swofford, D. L. (2002). PAUP\* Phylogenetic analysis using parsimony (\*and other methods). Version 4  
622 beta. *Sunderland, MA: Sinauer Associates Inc, software*.
- 623 Tamura, K., Stecher, G., Peterson, D., Filipski, A., and Kumar, S. (2013). MEGA6: molecular evolutionary  
624 genetics analysis version 6.0. *Molecular biology and evolution*, 30(12):2725–2729.
- 625 Timmermans, M., Roelofs, D., Mariën, J., and Van Straalen, N. (2008). Revealing pancrustacean  
626 relationships: Phylogenetic analysis of ribosomal protein genes places Collembola (springtails) in  
627 a monophyletic Hexapoda and reinforces the discrepancy between mitochondrial and nuclear DNA  
628 markers. *BMC Evolutionary Biology*, 8(1):83.
- 629 Whitfield, J. B. (1997). Molecular and morphological data suggest a single origin of the polydnaviruses  
630 among braconid wasps. *Naturwissenschaften*, 84(11):502–507.
- 631 Winterton, S. and De Freitas, S. (2006). Molecular phylogeny of the green lacewings (Neuroptera:  
632 Chrysopidae). *Austral Entomology*, 45(3):235–243.
- 633 Wool, I. G. (1979). The structure and function of eukaryotic ribosomes. *Annual review of biochemistry*,  
634 48(1):719–754.
- 635 Zhang, C., Stadler, T., Klopstein, S., Heath, T., and Ronquist, F. (2015). Total-evidence dating under the  
636 fossilized birth–death process. *Systematic Biology*, 65:228–249.

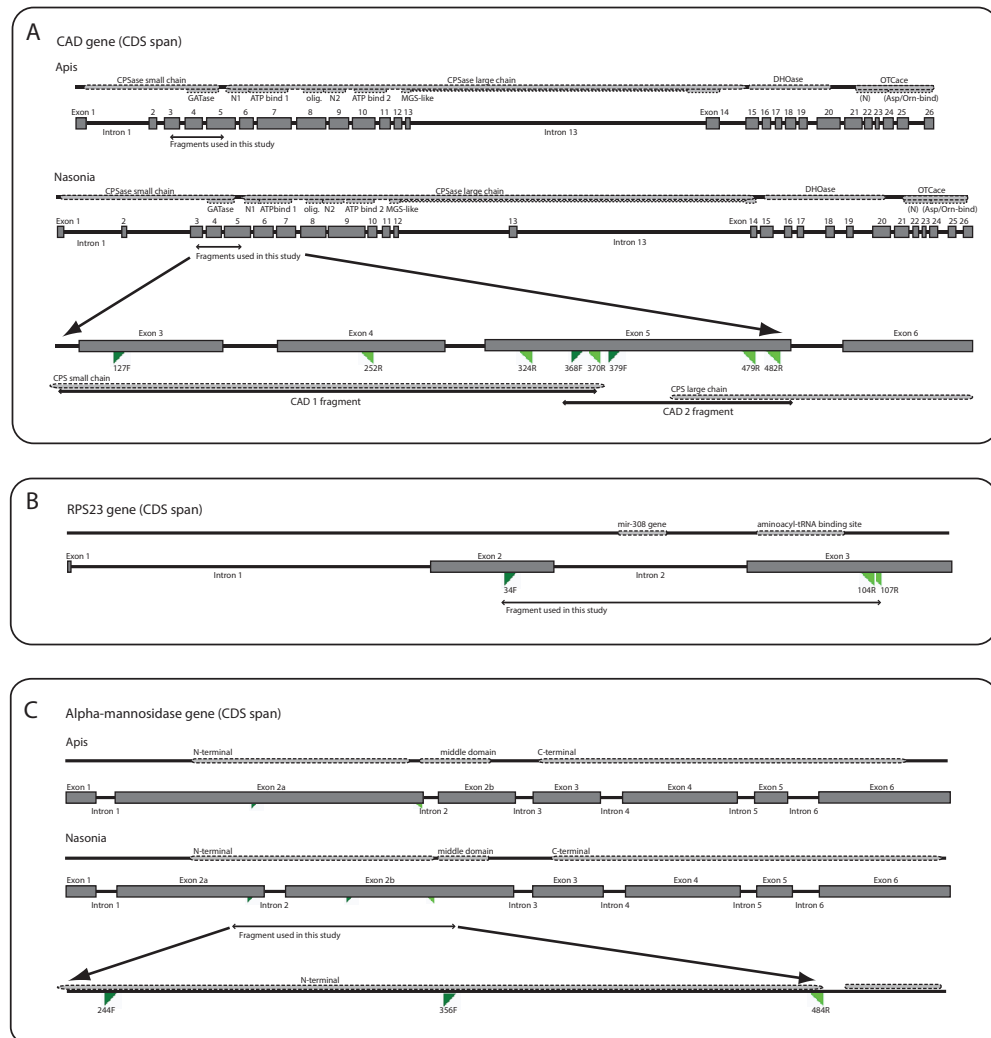


**Figure 1.** Diagrammatic gene maps for: **(A)** carbamoyl-phosphate synthetase-aspartate transcarbamoylase-dihydroorotase (*CAD*); **(B)** ribosomal protein S23 (*RPS23*); and **(C)** alpha-mannosidase II (*AM2*). Dotted lines mark protein domains and features. For *CAD* and *AM2*, *Apis* and *Nasonia* gene diagrams are shown individually as references due to substantial differences in exon locations. The bottom diagram in each gene map depicts the regions amplified in this study. In *CAD*, intron 13 in *Nasonia* has been scaled down due to an incomplete sequence in the GenBank entry. Primers are named according to the amino acid position in the *Apis mellifera* protein. Forward primers are in dark green and reverse primers in light green. See Table S2 for primer combinations. Abbreviations: *CPS*, carbamoyl-phosphate synthase; *GAT*, glutamine aminotransferase; *DHO*, dihydroorotase; *MGS*, methylglyoxal-like; *OTC*, ornithine carbamoyltransferase; *SNI*, N-terminal of subunit 1 in CPS large chain; *N2*, N-terminal of subunit 2 in CPS large chain; olig., oligomerization domain.

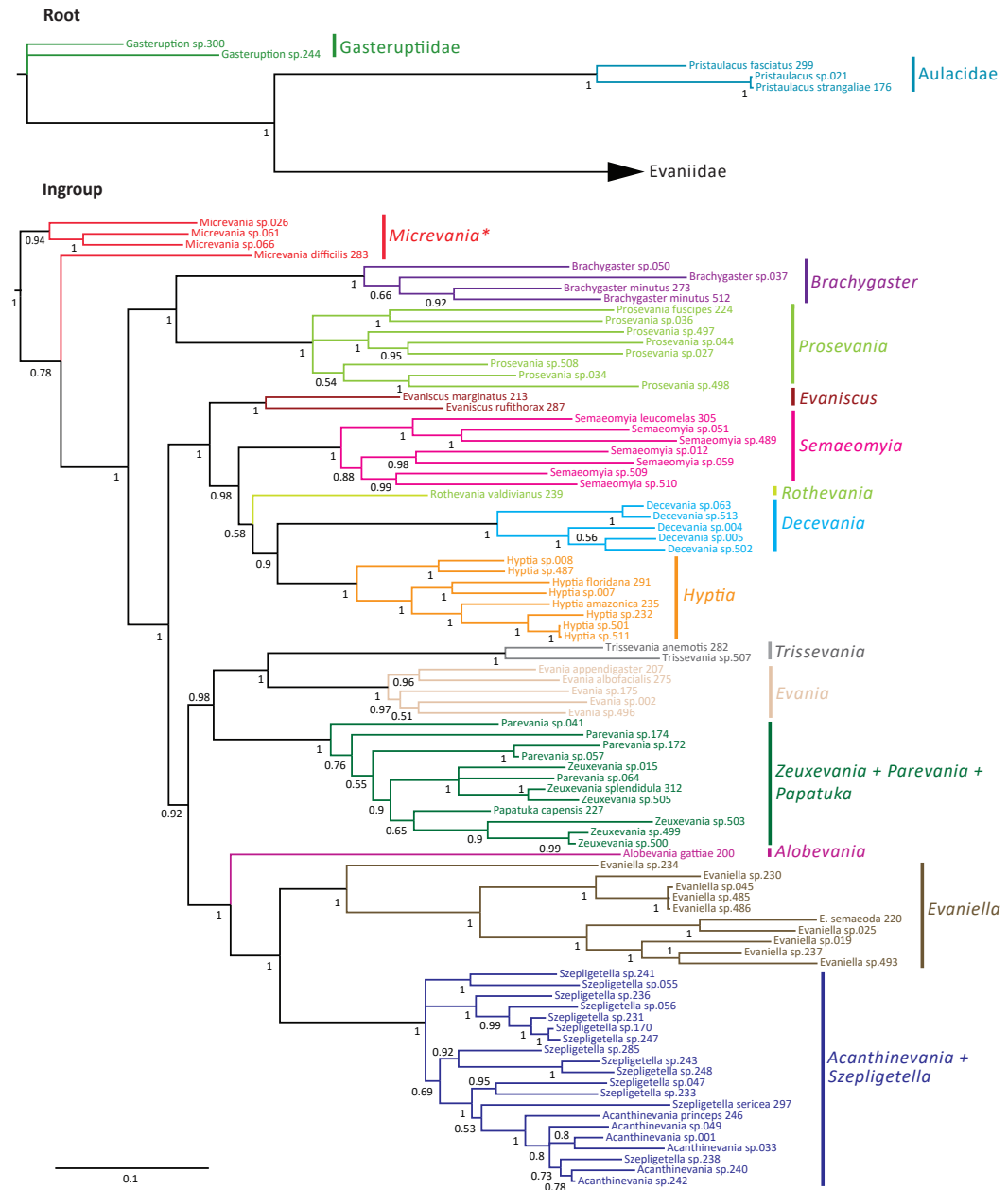


**Figure 2.** Bayesian analysis of phylogenetic relationships among Evaniidae. The outgroups were removed and placed above the ingroup tree for better visualization (the scale has been retained). Posterior probabilities are listed beside each clade.

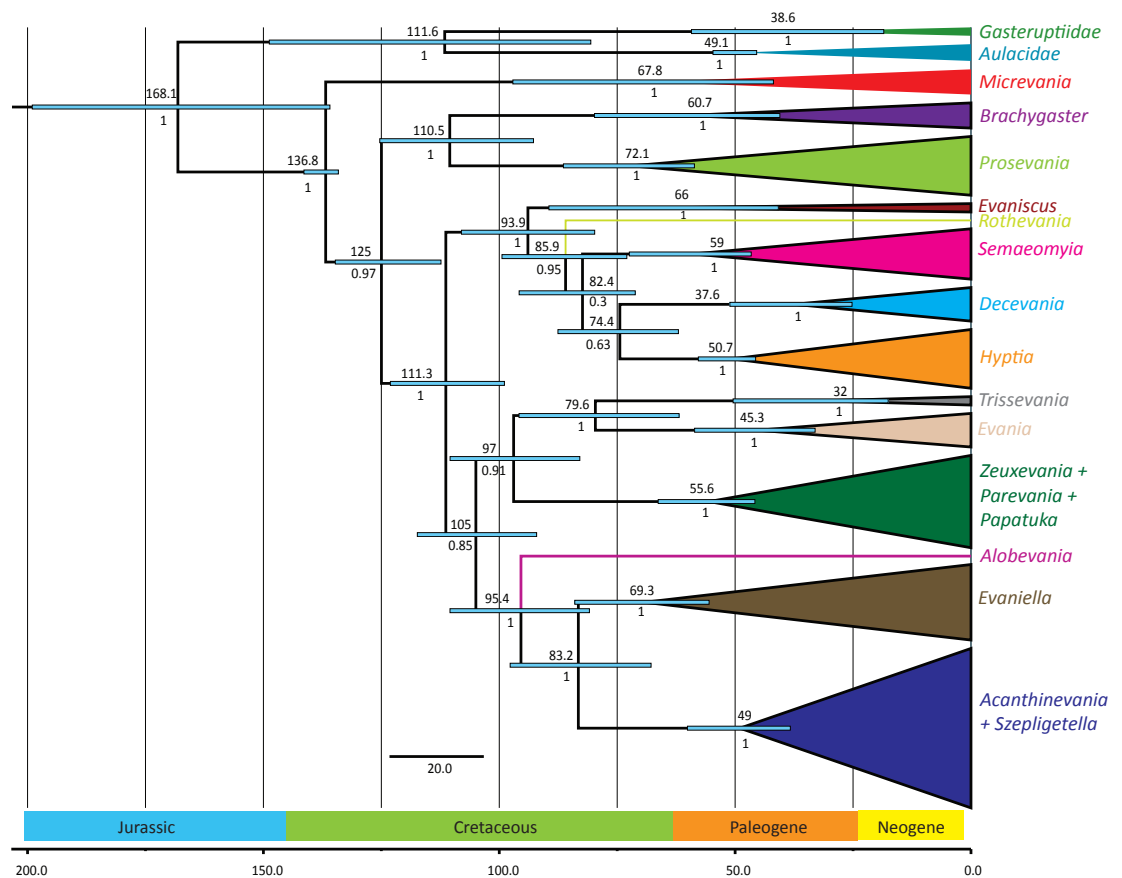


**Figure 3.** Simplified chronogram showing estimated divergence times for Evaniidae with six fossil calibrations and maximum clade ages under a lognormal distribution. Monophyletic genera have been collapsed for better visualization of the divergence estimations of the major clades. The blue bars indicate the 95% highest posterior density interval (HDI, also listed in Table 1). The scale is in millions of years. Mean age is listed above each clade and posterior probabilities are listed below .